

Optimal Matterwave Gravimetry

Michail Kritsotakis,¹ Stuart S. Szigeti,^{2,3} Jacob A. Dunningham,¹ and Simon A. Haine^{1,2}

¹*Department of Physics and Astronomy, University of Sussex, Brighton BN1 9QH, United Kingdom**

²*Department of Quantum Science, Research School of Physics and Engineering, The Australian National University, Canberra ACT 2601, Australia*

³*Department of Physics, Centre for Quantum Science, and Dodd-Walls Centre for Photonic and Quantum Technologies, University of Otago, Dunedin 9010, New Zealand*

We calculate quantum and classical Fisher informations for gravity sensors based on matterwave interference, and find that current Mach-Zehnder interferometry is not optimally extracting the full metrological potential of these sensors. We show that by making measurements that resolve either the momentum or the position we can considerably improve the sensitivity. We also provide a simple modification that is capable of more than doubling the sensitivity.

Atom interferometry is a leading inertial-sensing technology, having demonstrated state-of-the-art gravimetry [1–7] and gradiometry [8–14] measurements. Nevertheless, orders of magnitude improvement in sensitivity is required for applications in navigation [15] and mineral exploration [16], as well as improved tests of the equivalence principle [17–19] and quantum gravity [20, 21]. For the commonly-used Mach-Zehnder [i.e. Kasevich-Chu (KC)] configuration [22, 23], semiclassical calculations [24–27] reveal that the matterwave accrues relative phase $\phi = \mathbf{g} \cdot \mathbf{k}_L T_\pi^2$, where \mathbf{g} is the gravitational acceleration, $\hbar \mathbf{k}_L$ is the momentum separation of the two arms, and $2T_\pi$ is the total interrogation time. Assuming N uncorrelated particles, a population-difference measurement at the interferometer output yields sensitivity

$$\Delta g = \frac{1}{\sqrt{N} k_0 T_\pi^2}, \quad (1)$$

where k_0 is the component of \mathbf{k}_L aligned with \mathbf{g} . Equation (1) implies only four routes to improved sensitivity: (1) increase interrogation time, (2) increase the momentum separation of the arms (e.g. via large momentum transfer beam splitters [28–32]), (3) increase the atom flux, and/or (4) surpass the shot-noise limit with quantum correlations [33–37]. Although all routes are worth pursuing, each has unique limitations. For instance, size, weight, and power constraints limit both T_π and the maximum momentum transferrable via laser pulses. Additionally, evaporative-cooling losses and momentum width requirements constrain atom fluxes [38–42]. Increases with number-conserving feedback cooling are possible, but untested [43–45]. Finally, quantum-correlated states must be compatible with the requirements of high-precision metrology [5, 46–57] (e.g. high atom flux, low phase diffusion), and will only be advantageous if classical noise sources (e.g. [58, 59]) are sufficiently controlled to yield shot-noise-limited operation *prior* to quantum enhancement.

This assessment assumes that Eq. (1) is the *optimal* sensitivity. In this article, we prove this conventional wisdom false by showing that matterwave interferometers *can* attain better sensitivities than Eq. (1). Ultimately, the gravitational field affects the quantum state beyond the creation of a simple phase shift. We show this additional metrological potential via the quantum Fisher information (QFI), which determines the *best* possible sensitivity. We further determine the set of measurements required to attain this optimal sensitivity via the classical Fisher information (CFI). Our analysis reveals additional routes to improved sensitivity, such as variations in the measurement procedure and input source, and these should be considered when designing future matterwave gravimeters. We also present a modified interferometer that more than doubles the sensitivity for the same interrogation time and momentum separation.

The focus of this article is KC interferometry based on state-changing Raman transitions, although our results also hold for Bragg transitions [5] and Bloch oscillations [29] in the appropriate regime. A KC interferometer is schematically depicted in Fig. 1(a). At time $t = 0$ atoms with two internal states $|a\rangle$ and $|b\rangle$, initially in $|a\rangle$, are excited to an equal superposition of $|a\rangle$ and $|b\rangle$ via a coherent $\pi/2$ pulse. Atoms transferred to $|b\rangle$ also receive a momentum kick $\hbar k_0$. At $t = T_\pi$, a π pulse acts as a mirror, before the two matterwaves are interfered at $t = T = 2T_\pi$ by a second $\pi/2$ pulse.

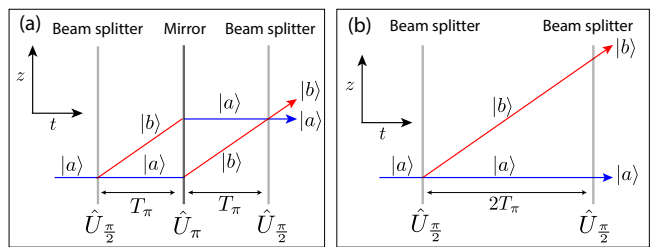


FIG. 1. Spacetime diagrams for (a) KC interferometry and (b) Ramsey interferometry (no mirror pulse), which are both sensitive to gravitational fields and accelerations.

* M.Kritsotakis@sussex.ac.uk

I. QFI FOR A PARTICLE IN A GRAVITATIONAL FIELD

The quantum Cramér-Rao bound (QCRB) gives a lower bound on the sensitivity [60]. For N uncorrelated particles this is $\Delta g^2 \geq 1/(NF_Q)$, where F_Q is the single-particle QFI [61–63], which for a pure single-particle state $|\Psi\rangle$ is

$$F_Q = 4 \left(\langle \partial_g \Psi | \partial_g \Psi \rangle - |\langle \Psi | \partial_g \Psi \rangle|^2 \right). \quad (2)$$

For the KC interferometer, semiclassical arguments give $|\Psi\rangle = \frac{1}{\sqrt{2}}(|a\rangle + e^{igk_0 T^2} |b\rangle)$ before the final beam splitter and a QFI $F_Q^{\text{sc}} = k_0^2 T_\pi^4$ [64], consistent with Eq. (1). However, this derivation treats the particle's motion semiclassically, neglecting the noncommutability of position and momentum. We account for this here. For the moment we consider only the centre of mass degrees of freedom. In the presence of a uniform gravitational field g acting along the z -axis, a particle of mass m in state $|\psi_0\rangle$ evolves to $|\psi(T)\rangle = \hat{U}_g |\psi_0\rangle$ after time T , where $\hat{U}_g = \exp[-\frac{iT}{\hbar}(\frac{\hat{p}^2}{2m} + mg\hat{z})]$. As shown in Appendix A, we can rewrite

$$\hat{U}_g = e^{-i\frac{T}{\hbar}\frac{\hat{p}^2}{2m}} e^{-ig\hat{G}_0(T)} e^{i\frac{mg^2 T^3}{12\hbar}}, \quad (3)$$

where

$$\hat{G}_0(T) = \frac{T}{\hbar} \left(\frac{T}{2} \hat{p}_z + m\hat{z} \right). \quad (4)$$

The QFI is

$$F_Q(T) = 4\text{Var}(G_0(T)) \quad (5a)$$

$$= \frac{T^4}{\hbar^2} \text{Var}(p_z) + \frac{4m^2 T^2}{\hbar^2} \text{Var}(z) + \frac{4mT^3}{\hbar^2} \text{Cov}(p_z, z), \quad (5b)$$

where the variances and covariance are evaluated with respect to $|\psi_0\rangle$. To compare Eq. (5a) and F_Q^{sc} , consider a state $|\psi_0\rangle$ with two well-defined peaks in momentum space separated by $\hbar k_0$, giving $\text{Var}(p_z) \approx (\hbar k_0)^2$. For sufficiently large k_0 and T such that $(\hbar k_0 T/2)^2 \gg m^2 \text{Var}(z)$, $mT\text{Cov}(p_z, z)$, the first term of Eq. (5b) dominates, and $F_Q(2T_\pi) \approx k_0^2 T_\pi^4 = F_Q^{\text{sc}}$. However, the additional terms in Eq. (5b) potentially allow sensitivities better than Eq. (1).

II. QFI FOR KC INTERFEROMETRY

Equation (5a) is *not* the QFI for a KC interferometer, as we must account for the internal state degrees of freedom as well as the action of the mirror pulse. The evolution is given by

$$\hat{U}_{\text{KC}} = \hat{U}_{\frac{\pi}{2}}^{\phi_3} \hat{U}_g(T_2) \hat{U}_\pi^{\phi_2} \hat{U}_g(T_1) \hat{U}_{\frac{\pi}{2}}^{\phi_1}, \quad (6)$$

where

$$\hat{U}_\theta^\phi = \hat{1} \cos\left(\frac{\theta}{2}\right) - i(|b\rangle\langle a| e^{i(k_0\hat{z}-\phi)} + \text{h.c.}) \sin\left(\frac{\theta}{2}\right) \quad (7)$$

governs the beam splitter and mirror dynamics. As shown in Appendix D, Eq. (7) is an excellent approximation to the beam splitting and mirror dynamics when the pulse duration is much shorter than the timescale for atomic motional dynamics. Here $T_{1(2)}$ are evolution times before(after) the π pulse and ϕ is the pulse phase, controlled via the relative phase of the two Raman lasers. The first $\pi/2$ pulse maps the initial state $|\Psi_0\rangle = |a\rangle|\psi_0\rangle$ to $|\Psi'_0\rangle = \hat{U}_{\frac{\pi}{2}}^{\phi_1}|\Psi_0\rangle = \frac{1}{\sqrt{2}}(|a\rangle - ie^{i(k_0\hat{z}-\phi_1)}|b\rangle)|\psi_0\rangle$, where $|\psi_0\rangle$ contains the initial state's motional degrees of freedom. As detailed in Appendix B,

$$|\Psi(T)\rangle = \hat{U}_{\text{KC}}|\Psi_0\rangle = \hat{U}_0 e^{-ig(\hat{G}_0(T) + \hat{G}_e)}|\Psi'_0\rangle, \quad (8)$$

where

$$\hat{G}_e = \hat{S}_z k_0 T_2^2, \quad (9a)$$

$$\hat{S}_z = \frac{1}{2} (|a\rangle\langle a| - |b\rangle\langle b|), \quad (9b)$$

$$\hat{U}_0 = \hat{U}_{\frac{\pi}{2}}^{\phi_3} e^{-i\frac{T_2}{\hbar}\frac{\hat{p}^2}{2m}} \hat{U}_\pi^{\phi_2} e^{-i\frac{T_1}{\hbar}\frac{\hat{p}^2}{2m}}, \quad (9c)$$

and $T = T_1 + T_2$, giving QFI

$$F_Q^{\text{KC}}(T) = 4\text{Var}(G_0(T)) + \frac{1}{4}k_0^2 (T^2 - 2T_2^2)^2, \quad (10)$$

where $\text{Var}(G_0(T))$ is taken with respect to $|\psi_0\rangle$. For $T_1 = T_2 = T_\pi$,

$$F_Q^{\text{KC}}(T) = 4\text{Var}(G_0(T)) + k_0^2 T_\pi^4. \quad (11)$$

Since $\text{Var}(G_0(T)) \geq 0$, this implies $F_Q^{\text{KC}} \geq F_Q^{\text{sc}}$, thereby permitting sensitivities better than Eq. (1).

III. CLASSICAL FISHER INFORMATION

Although the QFI gives the best possible sensitivity, it is silent on how to *achieve* this sensitivity. The attainable sensitivity for a particular measurement choice is given by the CFI, which quantifies the information contained in the probability distribution constructed from measurements of a particular observable, and necessarily depends upon this choice of observable. We calculate the CFI via

$$F_C(\hat{\Lambda}) = \int d\lambda \frac{[\partial_g P(\lambda)]^2}{P(\lambda)}, \quad (12)$$

where $P(\lambda)$ is the probability of obtaining result λ when the observable $\hat{\Lambda}$ is measured [61, 62]. The CFI is bounded by the QCRB $F_C \leq F_Q$, so a measurement that saturates this bound is the optimal measurement.

A. CFI for population-difference measurement

For the standard population-difference measurement at the KC interferometer output, $\hat{\Lambda} = \hat{S}_z$ and $F_C(\hat{S}_z) = \sum_{s=a,b} (\partial_g P_s)^2 / P_s$, where $P_s = \int dz |\langle s | \langle z | \Psi(T) \rangle|^2$. As

detailed in Appendix C, an analytic solution exists in this case. Specifically,

$$P_a = \frac{1}{2}(1 + |\mathcal{C}| \sin \alpha), \quad (13a)$$

$$P_b = \frac{1}{2}(1 - |\mathcal{C}| \sin \alpha), \quad (13b)$$

yielding

$$F_C(\hat{S}_z) = \frac{|\mathcal{C}|^2 \cos^2 \alpha}{1 - |\mathcal{C}|^2 \sin^2 \alpha} k_0^2 \left(\frac{T^2}{2} - T_1^2 \right)^2, \quad (14)$$

where

$$\mathcal{C} = \langle \psi_0 | e^{i \frac{k_0}{m} (T_2 - T_1) \hat{p}_z} | \psi_0 \rangle \equiv |\mathcal{C}| e^{i\vartheta}, \quad (15a)$$

$$\alpha = \phi_f - \phi_g + \vartheta, \quad (15b)$$

with $\phi_f = \frac{\hbar k_0^2}{2m} (T_2 - T_1)$ and $\phi_g = k_0 g (\frac{T^2}{2} - T_1^2)$. The contrast $|\mathcal{C}|$ is determined by the spatial overlap of the two output wavepackets, since $\frac{\hbar k_0}{m} (T_2 - T_1)$ is the spatial separation. This depends strongly on the time difference $T_2 - T_1$. For an initial Gaussian state $\langle z | \psi_0 \rangle = \exp(-z^2/2\sigma^2)/(\pi\sigma^2)^{1/4}$, $|\mathcal{C}| = \exp[-\frac{\hbar^2 k_0^2}{4m^2 \sigma^2} (T_2 - T_1)^2]$.

Figure 2(a) shows the time dependence of the QFI and $F_C(\hat{S}_z)$ for this initial Gaussian state. Here $t = T_1 + T_2$, we fix T_π so the mirror pulse always occurs at $t = T_\pi$, and the second beam splitter occurs instantaneously before measurement. Explicitly, if $t \leq T_\pi$, then $T_1 = t$, $T_2 = 0$, and the mirror pulse has no meaningful effect; if $t > T_\pi$ then $T_1 = T_\pi$ and $T_2 = t - T_\pi$. When T_1 and T_2 are significantly different, the spatial overlap of the two modes at the interferometer output is poor, so both the contrast and CFI are close to zero. However, $|\mathcal{C}| = 1$ when $T_1 = T_2$ and $F_C(\hat{S}_z) = F_Q^{\text{sc}} = k_0^2 T_\pi^4$, giving the same sensitivity as Eq. (1). This is still less than F_Q^{KC} , indicating that a different measurement could yield improved sensitivities.

B. CFI for momentum-distribution measurement

Now consider a measurement that distinguishes internal states *and* fully resolves the z -component of the final momentum distribution, such as reported in Ref. [65]. This measurement yields CFI

$$F_C(\hat{S}_z, \hat{p}_z) = \sum_{s=a,b} \int dp_z \frac{[\partial_g P_s(p_z)]^2}{P_s(p_z)}, \quad (16)$$

where $P_s(p_z) = |\langle s | \langle p_z | \Psi(T) \rangle|^2$. Although no analytic formula exists for $F_C(\hat{S}_z, \hat{p}_z)$, the probabilities can be determined by numerically solving the Schrödinger equation, and the CFI computed from finite differences of these probabilities [63]. This requires an explicit choice of g ; although we consider the sensitivity near $g = 0$ for all numerical calculations, a large offset in g is easily accounted for by adjusting the beam splitter phases, as in typical atomic gravimeters [41].

Figure 2(a) shows that $F_C(\hat{S}_z, \hat{p}_z)$ is significantly larger than $F_C(\hat{S}_z)$ and very close to F_Q^{KC} . Additionally, $F_C(\hat{S}_z, \hat{p}_z) \approx F_Q^{\text{KC}}$ even when T_1 and T_2 are vastly different. This is because $P_s(p_z)$ displays interference fringes that are not present in $P_s = \int dp_z P_s(p_z)$ when spatial overlap is poor.

The origin of the increased information in $F_C(\hat{S}_z, \hat{p}_z)$ compared with $F_C(\hat{S}_z)$ is easily understood. Additional to the CFI associated with population exchange (generated by \hat{G}_e), there is information due to a shift in the momentum distribution. Concretely, consider initial momentum distribution $P_0(p_z)$. Under gravity, $\hat{p}_z(t) = \hat{p}_z(0) + mgt$, so $P(p_z, t) = P_0(p_z - mgt)$, giving

$$\begin{aligned} F_C(p_z) &= \int dp_z \frac{[\partial_g P(p_z, t)]^2}{P(p_z, t)} \\ &= [\partial_g p_z(t)]^2 \int dp_z \frac{[\partial_{p_z} P_0(p_z)]^2}{P_0(p_z)} \\ &\equiv (mt)^2 F_C^{p_z}, \end{aligned} \quad (17)$$

where $F_C^{p_z}$ is the CFI associated with resolvable small shifts in the momentum distribution. For the initial Gaussian considered in Fig. 2(a), adding this additional CFI to $F_C(\hat{S}_z)$ gives $F_C(\hat{S}_z, \hat{p}_z)|_{2T_\pi} = F_Q^{\text{sc}} + 8(mT_\pi\sigma/\hbar)^2$, in perfect agreement with our numerics. Note that this additional information is *not* the result of a phase shift so, unlike a standard KC interferometer, it is *not* affected by additional phase noise.

Our simulations also find near-perfect correlations between internal and momentum states, so a measurement that only resolves momentum (and not \hat{S}_z) also has CFI approximating $F_C(\hat{S}_z, \hat{p}_z)|_{2T_\pi}$, since an atom's internal state is inferred from its final momentum. Our analysis therefore holds for interferometers that do not change internal states, such as Bragg-scattering-based interferometers, provided $\hbar k_0 \gg \delta p$, where δp is the wave packet's initial momentum width [5, 28]. In our simulations $\hbar k_0 \approx 14\delta p$.

C. CFI for position-distribution measurement

Although the momentum distribution cannot always be resolved, a measurement of the *position* distribution might be possible. Here the CFI is

$$F_C(\hat{S}_z, \hat{z}) = \sum_{s=a,b} \int dz \frac{[\partial_g P_s(z)]^2}{P_s(z)}, \quad (18)$$

where $P_s(z) = |\langle s | \langle z | \Psi(t) \rangle|^2$. Figure 2(a) shows this is slightly better than the population-difference measurement, although significantly worse than the momentum measurement. Arguing as before, since the position distribution shifts due to $\hat{z}(t) = \hat{z}(0) + \hat{p}_z(0)t/m + \frac{1}{2}gt^2$, the additional CFI is $(t^2/2)^2 F_C^z$, where $F_C^z = \int dz [\partial_z P(z)]^2 / P(z)$ is the CFI associated with resolvable

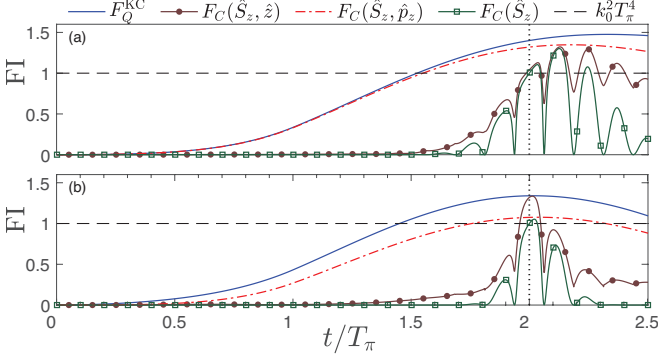


FIG. 2. Fisher information (FI) for $|\Psi(t)\rangle = \hat{U}_{\text{KC}}(t)|\Psi_0\rangle$, where $T_1 = t$ and $T_2 = 0$ for $t \leq T_\pi$, otherwise $T_1 = T_\pi$ and $T_2 = t - T_\pi$, with initial Gaussian motional state (a) $\langle z|\psi_0\rangle = \exp(-z^2/2\sigma^2)/(\pi\sigma^2)^{1/4}$ and (b) $\langle z|\psi_0\rangle = e^{-(\frac{1}{4}+i)z^2/2\sigma^2}/[\pi(2\sigma)^2]^{1/4}$. FI has units $k_0^2 T_\pi^4$, so when FI > 1 a given measurement scheme achieves a sensitivity better than that predicted by the semiclassical limit Eq. (1). The QFI F_Q^{KC} gives the maximum possible FI. Here $\sigma = 10L$ and $T_\pi = 100t_0$, whilst the length ($L = k_0^{-1}$) and time ($t_0 = m/\hbar k_0^2$) units depend on k_0 .

shifts in the position distribution. Since

$$\begin{aligned} \text{Var}(z(t)) &= \text{Var}(z(0)) + \frac{t^2}{m^2} \text{Var}(p_z(0)) \\ &\quad + \frac{t}{2m} \text{Cov}(p_z(0), z(0)), \end{aligned} \quad (19)$$

and $F_C^z = 1/\text{Var}(z)$ for Gaussian states, we obtain $F_C(\hat{S}_z, \hat{z})|_{2T_\pi} = F_Q^{\text{sc}} + 8(\sigma m T_\pi^2)^2/[(\sigma^2 m)^2 + (2\hbar T_\pi)^2]$ for the initial Gaussian considered in Fig. 2(a), in agreement with numerics.

We can increase $F_C(\hat{S}_z, \hat{z})$ with an initial state that decreases $\text{Var}(z(2T_\pi))$ at the interferometer output. This is not achieved by reducing $\text{Var}(z(0))$, but rather via an initial state with nontrivial correlations between position and momentum such that $\text{Cov}(\hat{p}_z, \hat{z})$ counteracts the wave packet's ballistic expansion. Figure 2(b) shows the QFI and CFI for initial state $\langle z|\psi_0\rangle = e^{-(\frac{1}{4}+i)z^2/2\sigma^2}/[\pi(2\sigma)^2]^{1/4}$. The imaginary term provides the position-momentum correlations and doubling the spatial width increases the ability of the wavepacket to be *focused*. This initial state could be engineered by applying a harmonic potential for a short duration (compared to motional dynamics), creating phase gradient $\psi(z) \rightarrow \psi(z)e^{-iz^2/\sigma_t^2}$, for constant σ_t which depends on trap frequency and duration [66]. Then $F_C(\hat{S}_z, \hat{z})$ saturates the QCRB at $T_1 = T_2$, at the cost of reduced $F_C(\hat{S}_z, \hat{p}_z)$.

IV. OPTIMUM MEASUREMENTS

Since measurements in different bases yield different sensitivities, is there an accessible measurement basis

that saturates the QCRB? Our above analysis suggests yes and, depending on the initial state, this optimum basis lies somewhere *between* position and momentum. We confirm this intuition by revisiting a particle in a gravitational field. We rewrite

$$|\psi(t)\rangle = \hat{U}_g|\psi_0\rangle = \exp(-ig\hat{G}'_0(t))|\psi_0(t)\rangle, \quad (20)$$

where

$$\hat{G}'_0(t) = \hat{U}_p \hat{G}_0(t) \hat{U}_p^\dagger = \frac{t}{\hbar}(m\hat{z} - \frac{1}{2}\hat{p}_z t), \quad (21)$$

$\hat{U}_p = \exp[-it\mathbf{p}^2/(2m\hbar)]$, and $|\psi_0(t)\rangle = \hat{U}_p|\psi_0\rangle$ describes free-particle evolution. We can interpret $\hat{G}'_0(t)$ as the generator of displacements in $\hat{Q} = c_1\hat{z} + c_2\hat{p}_z$, where the coefficients c_i are real and chosen such that $[\hat{G}'_0(t), \hat{Q}] = i$. Hence, the probability distribution $|\langle q|\psi(t)\rangle|^2 = |\langle q - g|\psi_0(t)\rangle|^2$, where $\hat{Q}|q\rangle = q|\hat{q}\rangle$. If $|\langle q|\psi_0(t)\rangle|^2$ is Gaussian, then measurements of \hat{Q} saturate the QCRB, since $[\hat{G}'_0(t), \hat{Q}] = i$ implies

$$F_C(\hat{Q}) = \frac{1}{\text{Var}(Q)} = 4\text{Var}(G'_0(t)) = F_Q. \quad (22)$$

To measure \hat{Q} , we mix \hat{z} and \hat{p}_z by applying the potential $V(z) = \frac{1}{2}m\omega^2 z^2$, since $\hat{z}(t) = \hat{z}(0) \cos \omega t + [\hat{p}(0)/m\omega] \sin \omega t$. Subsequently measuring position yields a combination of position and momentum information. This scheme could be implemented using the following procedure:

1. At $t = 2T_\pi$, apply the unitary $\hat{U}_s = |a\rangle\langle a| + |b\rangle\langle b|e^{-ik_0\hat{z}}$, which removes any momentum mismatch between the two modes. A state-selective Bragg transition achieves this.
2. Then apply the potential $V(z) = \frac{1}{2}m\omega^2(z - z_0)^2$, where $z_0 = \hbar k_0 T_\pi / m$ is the matterwave's centre-of-mass displacement at the interferometer output.
3. Finally, at some later time, we apply a beam splitter $\hat{U}_{\text{BS}} = \frac{1}{\sqrt{2}}[\hat{1} + (|a\rangle\langle b| - \text{h.c.})]$ immediately before measurement.

Figure 3 shows $F_C(\hat{S}_z, \hat{z})$ and $F_C(\hat{S}_z, \hat{p}_z)$ for this scheme. Both CFIs oscillate between F_Q^{sc} and the QFI, so a measurement in either the position or momentum basis saturates the QCRB if made at the appropriate time. This improved sensitivity *does* increase the interferometer time. However, the period of CFI oscillations is negligible compared to T_π for sufficiently large ω .

V. IMPROVED INTERFEROMETRY

In KC interferometry, the π pulse ensures that the wavepackets spatially overlap at $t = 2T_\pi$. However, Fig. 2 and Fig. 3 reveal that spatial overlap is *not* required for a momentum measurement, making the mirror pulse unnecessary. More interestingly, removing the

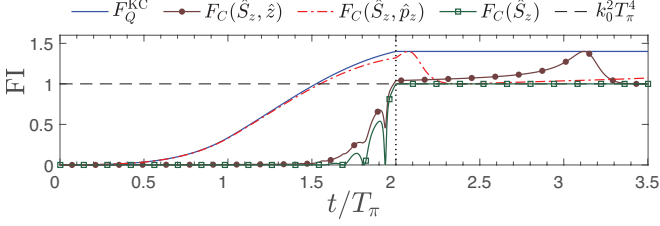


FIG. 3. Fisher information (FI) $|\Psi(t)\rangle = \hat{U}_{\text{KC}}(t)|\psi_0\rangle$, where $T_1 = t$ and $T_2 = 0$ for $t \leq T_\pi$, otherwise $T_1 = T_\pi$ and $T_2 = t - T_\pi$, with a harmonic potential applied at $t = 2T_\pi$ and initial Gaussian motional state $\langle z|\psi_0\rangle = \exp(-z^2/2\sigma^2)/(\pi\sigma^2)^{1/4}$. We artificially turned off gravity at $t = 2T_\pi$ (which holds F_Q^{KC} constant) to clearly show the effect of harmonic trapping. Specifically, the application of this harmonic potential can be used to saturate the QCRB with either a position-distribution or momentum-distribution measurement. Here $\sigma = 10L$, $T_\pi = 100t_0$, and $\omega = 3\pi/(2T_\pi)$. FI has units $k_0^2T_\pi^4$, and length ($L = k_0^{-1}$) and time ($t_0 = m/\hbar k_0^2$) units depend on k_0 .

π pulse significantly increases the spatial separation, and therefore the QFI, for the same interrogation time. More precisely, setting $T_1 = 2T_\pi$ and $T_2 = 0$ in Eq. (10) gives $F_Q(T) = 4\text{Var}(G_0(T)) + 4k_0^2T_\pi^4$, an increase of $3F_Q^{\text{sc}}$ over symmetric KC interferometry.

We numerically solved the Schrödinger equation for the mirrorless Mach-Zehnder (i.e. Ramsey) configuration [Fig. 1(b)]. Figure 4(a) shows that a momentum measurement is always nearly optimal, and at $t = 2T_\pi$, $F_C(\hat{S}_z, \hat{p}_z)/F_Q^{\text{sc}} \approx 4.4$. Unfortunately, this improved sensitivity has a price: A lack of spatial overlap means that information is encoded in high-frequency interference fringes in the momentum distribution, requiring high-resolution momentum measurements. Following Refs. [67–71], we model imperfect resolution by convolving the momentum distribution at $t = 2T_\pi$ with a Gaussian of width σ_p before constructing $F_C(\hat{S}_z, \hat{p}_z)$ [Fig. 4(b)]. This imperfect resolution may be due to limitations on the detection system, or other sources of classical noise. The mirrorless configuration is considerably more sensitive to imperfect momentum resolution than KC interferometry, where $F_C(\hat{S}_z, \hat{p}_z)$ begins to degrade only when σ_p is comparable to the initial wavepacket's momentum width. Furthermore, in the limit of a “bad” momentum measurement ($\sigma_p \rightarrow \infty$), the CFI goes to zero, whereas the CFI for KC interferometry approaches F_Q^{sc} . Nevertheless, if high-resolution measurements are available (or actively developed), as reported in Ref. [72] for instance, our result suggests that pursuing a mirrorless configuration could yield substantial sensitivity gains.

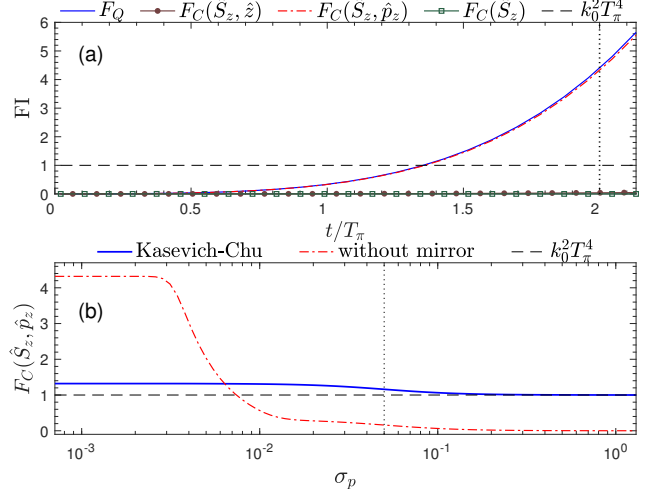


FIG. 4. (a) FI of the mirrorless configuration for the same initial state and parameters as Fig. 2(a). We normalize time by $T_\pi = 100t_0$ only for comparison with Fig. 2. Note that $F_C(\hat{S}_z)$ and $F_C(\hat{S}_z, \hat{z})$ are almost zero throughout the entire evolution, since there is no spatial overlap of the wavepackets and consequently no interference in P_s or the position distribution. (b) $F_C(\hat{S}_z, \hat{p}_z)$ constructed from convolving probabilities with a Gaussian of width σ_p (units $\hbar k_0$). The vertical line marks the initial state's momentum width: $\delta p = \hbar/\sqrt{2}\sigma \approx 0.07\hbar k_0$. FI is in units of $k_0^2T_\pi^4$.

VI. DISCUSSION AND OUTLOOK

An important experimental consideration is achieving high-resolution momentum measurements. Time-of-flight imaging is a standard technique, where ballistic expansion converts the momentum distribution into a position distribution [73, 74]. However, the expansion time needed for sufficient momentum resolution might be significantly longer than the interrogation time, in which case longer interrogation times are a better route to improved sensitivities. Bragg spectroscopy is perhaps a more promising approach [75, 76].

Reference [7] reports state-of-the-art gravimetry with a Bose-Einstein condensate (BEC), well-described by a pure motional state, and parameters: $\sigma = 40\mu\text{m}$, $T_\pi = 130\text{ms}$, $k_0 = 1.6 \times 10^7 \text{ m}^{-1}$, and $\delta p_z = 0.18\hbar k_0$. We estimate that $4\text{Var}(G_0(T)) \approx 7\%$ of F_Q^{sc} , so there is little gain in making optimal measurements [Eq. (11)]. However, $4\text{Var}(G_0(T)) \sim F_Q^{\text{sc}}$ if σ or δp_z were increased by an order of magnitude. This suggests that creating initial (pure) states with large spatial extent, such as quasi-continuous atom lasers [42, 77], could yield substantial sensitivity gains. Additionally, compact and/or high-bandwidth devices could benefit from optimal measurements, since shorter interrogation times increase $\text{Var}(G_0(T))$ relative to F_Q^{sc} .

For KC interferometers with thermal (mixed) states, Eq. (11) is only an upper bound for the QFI [61]. A calcu-

lation of F_Q and F_C for thermal sources gives values substantially greater than F_Q^{sc} [78], in qualitative agreement with our above analysis, showing that current thermal-atom gravimetry is suboptimal. However, the QFI and CFI are also smaller than Eq. (11) for thermal sources, suggesting that BECs possess metrological potential beyond what is possible with thermal sources.

Our approach to evaluating matterwave interferometry could significantly influence the design of future state-of-the-art gravimeters. Typical interferometer design assumes a particular form for the measurement signal (e.g., the population difference at the output varies sinusoidally with g) and looks no further if there is agreement with simple ‘best case’ formulae such as Eq. (1). In contrast, a Fisher analysis gives the full metrological potential of *any* given dynamical scheme without enforcing such *a priori* assumptions by simply considering the available data. Our matterwave gravimetry analysis opens up new routes to improved sensitivity – beyond those few implied by Eq. (1). This includes engineering states with high QFI [i.e. large $\text{Var}(G_0(T))$] and improving information extraction at the interferometer output. Our mirrorless scheme gives a substantial sensitivity boost if high-resolution momentum measurements are available. For [7], this momentum resolution is $10^{-4}\hbar k_0$, achievable by further developing the $2 \times 10^{-4}\hbar k_0$ resolution measurement of [72]. A Fisher analysis could prove beneficial for evaluating other atom-interferometer-based sensors which produce a complicated output signal, such as schemes utilizing Kapitza-Dirac scattering [79–84] or propagation in crossed waveguides [85].

ACKNOWLEDGMENTS

We acknowledge fruitful discussions with John Close, Chris Freier, Paul Griffin, Kyle Hardman, Guglielmo Tino, Nicola Poli, Samuel Nolan, Augusto Smerzi, and Nicholas Robins. MK and JAD received funding from UK EPSRC through the Networked Quantum Information Technology (NQIT) Hub, grant reference EP/M013243/1. SSS received funding from an Australia Awards-Endeavour Research Fellowship, the Dodd-Walls Centre for Photonic and Quantum Technologies, and Australian Research Council projects DP160104965 and DP150100356. SAH was supported by the European Union’s Horizon 2020 research and innovation programme under the Marie Skłodowska-Curie grant agreement No. 704672.

Appendix A: QFI of a particle in a gravitational field

Here we give a more detailed derivation of Eq. (5a). Approximating the gravitational field as a linear potential $mg\hat{z}$, the state of the particle after time T is

$$|\Psi(T)\rangle = \hat{U}_g(T)|\Psi_0\rangle, \text{ where}$$

$$\hat{U}_g(T) = \exp\left[-\frac{iT}{\hbar}\left(\frac{\hat{p}^2}{2m} + mg\hat{z}\right)\right]. \quad (\text{A1})$$

In order to isolate the contribution due to the gravitational field g , we make use of the Baker-Campbell-Hausdorff (BCH) lemma:

$$e^{\hat{X}+\hat{Y}} = e^{\hat{X}}e^{\hat{Y}}e^{-\frac{1}{2}[\hat{X},\hat{Y}]}e^{\frac{1}{6}(2[\hat{Y},[\hat{X},\hat{Y}]]+[\hat{X},[\hat{X},\hat{Y}]])}, \quad (\text{A2})$$

where \hat{X} and \hat{Y} are operators satisfying the commutation relations

$$[[[\hat{X},\hat{Y}],\hat{X}],\hat{X}] = [[[[\hat{X},\hat{Y}],\hat{X}],\hat{Y}] = [[[[\hat{X},\hat{Y}],\hat{Y}],\hat{Y}] = 0. \quad (\text{A3})$$

This is true for $\hat{X} = -\frac{iT}{\hbar}\frac{\hat{p}^2}{2m}$ and $\hat{Y} = -\frac{iT}{\hbar}mg\hat{z}$, where

$$[\hat{X},\hat{Y}] = \frac{igT^2}{\hbar}\hat{p}_z, \quad (\text{A4a})$$

$$[\hat{Y},[\hat{X},\hat{Y}]] = \frac{img^2T^3}{\hbar}, \quad (\text{A4b})$$

$$[\hat{X},[\hat{X},\hat{Y}]] = 0. \quad (\text{A4c})$$

Thus, Eq. (A2) gives:

$$e^{-\frac{iT}{\hbar}\left(\frac{\hat{p}^2}{2m}+mg\hat{z}\right)} = e^{-\frac{iT}{\hbar}\frac{\hat{p}^2}{2m}}e^{-\frac{iT}{\hbar}mg\hat{z}}e^{-\frac{igT^2}{2\hbar}\hat{p}_z}e^{\frac{img^2T^3}{3\hbar}}. \quad (\text{A5})$$

We use Eq. (A2) again with the choice $\hat{X} = -\frac{iT}{\hbar}mg\hat{z}$ and $\hat{Y} = -\frac{igT^2}{2\hbar}\hat{p}_z$, where $[\hat{X},\hat{Y}] = -\frac{img^2T^3}{2\hbar}$, which allows us to combine $\exp[-i(T/\hbar)mg\hat{z}]$ and $\exp[-igT^2\hat{p}_z/(2\hbar)]$ into a single exponential:

$$e^{-\frac{iT}{\hbar}mg\hat{z}}e^{-\frac{igT^2}{2\hbar}\hat{p}_z} = e^{-ig\hat{G}_0(T)}e^{-\frac{img^2T^3}{4\hbar}}, \quad (\text{A6})$$

where $\hat{G}_0(T) = \frac{T}{\hbar}(\frac{T}{2}\hat{p}_z + m\hat{z})$. Thus, the evolution operator $\hat{U}_g(T)$ can be written as:

$$\begin{aligned} \hat{U}_g(T) &= e^{-\frac{iT}{\hbar}\left(\frac{\hat{p}^2}{2m}+mg\hat{z}\right)} \\ &= e^{-i\frac{T}{\hbar}\frac{\hat{p}^2}{2m}}e^{-ig\hat{G}_0(T)}e^{i\frac{mg^2T^3}{12\hbar}}. \end{aligned} \quad (\text{A7})$$

We can ignore $\exp[img^2T^3/(12\hbar)]$, since this is just a global phase factor, and so the state of the particle after time T is

$$|\Psi(T)\rangle = e^{-\frac{iT}{\hbar}\frac{\hat{p}^2}{2m}}e^{-ig\hat{G}_0(T)}|\Psi_0\rangle. \quad (\text{A8})$$

It is now simple to compute the derivative of $|\Psi(T)\rangle$ with respect to g :

$$|\partial_g\Psi(T)\rangle = -ie^{-\frac{iT}{\hbar}\frac{\hat{p}^2}{2m}}\hat{G}_0(T)e^{-ig\hat{G}_0(T)}|\Psi_0\rangle. \quad (\text{A9})$$

Consequently,

$$\langle\partial_g\Psi(T)|\partial_g\Psi(T)\rangle = \langle\Psi_0|\hat{G}_0(T)^2|\Psi_0\rangle, \quad (\text{A10a})$$

$$\langle\Psi(T)|\partial_g\Psi(T)\rangle = -i\langle\Psi_0|\hat{G}_0(T)|\Psi_0\rangle. \quad (\text{A10b})$$

Substituting these into Eq. (2) gives our final expression for the QFI, Eq. (5a).

Appendix B: QFI of a particle after KC interferometry

Here we provide a derivation of Eq. (10). The total evolution of a particle due to KC interferometry is given by the unitary operator

$$\hat{U}_{\text{KC}} = \hat{U}_{\frac{\pi}{2}}^{\phi_3} \hat{U}_g(T_2) \hat{U}_{\pi}^{\phi_2} \hat{U}_g(T_1) \hat{U}_{\frac{\pi}{2}}^{\phi_1}, \quad (\text{B1})$$

where $\hat{U}_{\frac{\pi}{2}}^{\phi}$ and \hat{U}_{π}^{ϕ} denote $\pi/2$ (50/50 beam splitting) and π (mirror) pulses, respectively, and the evolution due to the gravitational field, $\hat{U}_g(T)$, was derived above [see Eq. (A7)]. This assumes that the $\pi/2$ and π pulses are instantaneous (strictly, occur on times much shorter than the interrogation times T_1 and T_2).

To begin, the final $\pi/2$ pulse does not change the QFI, whilst the first $\pi/2$ pulse simply gives a new initial state for the particle [see Eq. (7)]:

$$\begin{aligned} |\Psi'_0\rangle &= \hat{U}_{\frac{\pi}{2}}^{\phi_1} |\Psi_0\rangle \\ &= \frac{1}{\sqrt{2}} \left(|\psi_0\rangle |a\rangle - ie^{i(k_0\hat{z}-\phi_1)} |\psi_0\rangle |b\rangle \right), \end{aligned} \quad (\text{B2})$$

where $|\Psi_0\rangle = |a\rangle |\psi_0\rangle$ and ϕ_1 is the phase of this first laser

pulse. Consequently, the QFI can be computed from the product of operators $\hat{U}_g(T_2) \hat{U}_{\pi}^{\phi_2} \hat{U}_g(T_1)$, provided expectations are taken with respect to the state $|\Psi'_0\rangle$.

As in Appendix A, our goal is to isolate the g -dependence of the evolution. We first consider the product $\hat{U}_g(T_2) \hat{U}_{\pi}^{\phi_2}$, where [see Eq. (7)]

$$\hat{U}_{\pi}^{\phi_2} = -i \left(e^{-i(k_0\hat{z}-\phi_2)} |a\rangle\langle b| + e^{i(k_0\hat{z}-\phi_2)} |b\rangle\langle a| \right), \quad (\text{B3})$$

and ϕ_2 is the phase of this mirror pulse. The BCH lemma Eq. (A2) implies that

$$\begin{aligned} e^{\hat{X}} e^{\hat{Y}} e^{-\frac{1}{2}[\hat{X}, \hat{Y}]} e^{\frac{1}{6}(2[\hat{Y}, [\hat{X}, \hat{Y}]] + [\hat{X}, [\hat{X}, \hat{Y}]])} \\ = e^{\hat{Y}} e^{\hat{X}} e^{\frac{1}{2}[\hat{X}, \hat{Y}]} e^{-\frac{1}{6}(2[\hat{X}, [\hat{X}, \hat{Y}]] + [\hat{Y}, [\hat{X}, \hat{Y}]])}. \end{aligned} \quad (\text{B4})$$

The application of Eq. (B4) with $\hat{X} = -ig\hat{G}_0(T_2)$ and $\hat{Y}_{\pm} = \pm ik_0\hat{z}$ gives

$$e^{-ig\hat{G}_0(T_2)} e^{\pm ik_0\hat{z}} = e^{\pm ik_0\hat{z}} e^{-ig\hat{G}_0(T_2)} e^{\mp i\frac{1}{2}gk_0T_2^2}, \quad (\text{B5})$$

where we have used $[\hat{X}, \hat{Y}_{\pm}] = \mp igk_0T_2^2/2$. Therefore, after neglecting the global phase factor $\exp[img^2T_2^3/(12\hbar)]$ in $\hat{U}_g(T)$:

$$\begin{aligned} \hat{U}_g(T_2) \hat{U}_{\pi}^{\phi_2} &= -ie^{-\frac{iT_2}{\hbar}\frac{\hat{p}^2}{2m}} \left(e^{-i(k_0\hat{z}-\phi_2)} e^{-ig\hat{G}_0(T_2)} e^{i\frac{1}{2}gk_0T_2^2} |a\rangle\langle b| + e^{i(k_0\hat{z}+\phi_2)} e^{-ig\hat{G}_0(T_2)} e^{-i\frac{1}{2}gk_0T_2^2} |b\rangle\langle a| \right) \\ &= -ie^{-\frac{iT_2}{\hbar}\frac{\hat{p}^2}{2m}} \left(e^{-i(k_0\hat{z}-\phi_2)} e^{i\frac{1}{2}gk_0T_2^2} |a\rangle\langle b| + e^{i(k_0\hat{z}+\phi_2)} e^{-i\frac{1}{2}gk_0T_2^2} |b\rangle\langle a| \right) e^{-ig\hat{G}_0(T_2)}. \end{aligned} \quad (\text{B6})$$

Note that $\hat{G}_0(T_2)$ acts only on the motional state of the particle and therefore commutes with any operators that act on the internal states $|a\rangle$ and $|b\rangle$.

Now internal states $|a\rangle$ and $|b\rangle$ are the eigenvectors of $\hat{S}_z = \frac{1}{2}(|a\rangle\langle a| - |b\rangle\langle b|)$ satisfying $\hat{S}_z|a\rangle = \frac{1}{2}|a\rangle$ and $\hat{S}_z|b\rangle = -\frac{1}{2}|b\rangle$. Therefore, for an arbitrary operator \hat{O} which solely acts on the motional state of the particle:

$$e^{\hat{O}\hat{S}_z} |a\rangle = e^{\frac{1}{2}\hat{O}} |a\rangle, \quad e^{\hat{O}\hat{S}_z} |b\rangle = e^{-\frac{1}{2}\hat{O}} |b\rangle. \quad (\text{B7})$$

This allows us to write

$$\langle a| e^{-i\frac{1}{2}gk_0T_2^2} = \langle a| e^{-igk_0T_2^2\hat{S}_z} = \langle a| e^{-ig\hat{G}_e}, \quad (\text{B8a})$$

$$\langle b| e^{i\frac{1}{2}gk_0T_2^2} = \langle b| e^{-igk_0T_2^2\hat{S}_z} = \langle b| e^{-ig\hat{G}_e}, \quad (\text{B8b})$$

where $\hat{G}_e = k_0T_2^2\hat{S}_z$. Therefore,

$$\hat{U}_g(T_2) \hat{U}_{\pi}^{\phi_2} = e^{-\frac{iT_2}{\hbar}\frac{\hat{p}^2}{2m}} \hat{U}_{\pi}^{\phi_2} e^{-ig\hat{G}_e} e^{-ig\hat{G}_0(T_2)}. \quad (\text{B9})$$

Next, we again use Eq. (B4) with $\hat{X} = -ig\hat{G}_0(T_2)$ and

$\hat{Y} = -\frac{iT_1}{\hbar}\frac{\hat{p}^2}{2m}$, where

$$[\hat{X}, \hat{Y}] = -\frac{igT_1T_2}{\hbar} \hat{p}_z, \quad (\text{B10a})$$

$$[\hat{X}, [\hat{X}, \hat{Y}]] = -\frac{img^2T_1T_2^2}{\hbar}, \quad (\text{B10b})$$

to obtain

$$\begin{aligned} e^{-ig\hat{G}_0(T_2)} e^{-i\frac{T_1}{\hbar}\frac{\hat{p}^2}{2m}} \\ = e^{-i\frac{T_1}{\hbar}\frac{\hat{p}^2}{2m}} e^{-ig\hat{G}_0(T_2)} e^{-ig\frac{T_1T_2}{\hbar}\hat{p}_z} e^{i\frac{m}{2\hbar}g^2T_1T_2^2}, \end{aligned} \quad (\text{B11})$$

and therefore (ignoring the global phase factor $\exp[img^2T_1T_2^2/(2\hbar)]$)

$$\begin{aligned} \hat{U}_g(T_2) \hat{U}_{\pi}^{\phi_2} \hat{U}_g(T_1) &= e^{-i\frac{T_2}{\hbar}\frac{\hat{p}^2}{2m}} \hat{U}_{\pi}^{\phi_2} e^{-ig\hat{G}_e} e^{-i\frac{T_1}{\hbar}\frac{\hat{p}^2}{2m}} e^{-ig\hat{G}_0(T_2)} \\ &\times e^{-ig\frac{T_1T_2}{\hbar}\hat{p}_z} e^{-ig\hat{G}_0(T_1)}. \end{aligned} \quad (\text{B12})$$

We combine the final three exponentials into one using Eq. (A2):

$$\begin{aligned} \hat{U}_g(T_2) \hat{U}_{\pi}^{\phi_2} \hat{U}_g(T_1) \\ = e^{-i\frac{T_2}{\hbar}\frac{\hat{p}^2}{2m}} \hat{U}_{\pi}^{\phi_2} e^{-i\frac{T_1}{\hbar}\frac{\hat{p}^2}{2m}} e^{-ig(\hat{G}_0(T) + \hat{G}_e)}, \end{aligned} \quad (\text{B13})$$

where $T = T_1 + T_2$ and we have neglected all the global phases produced during the calculation.

Including the first and second $\pi/2$ pulses (although the second pulse is *not* needed for calculating the QFI), we arrive at the following simplified expression for the full KC interferometer evolution:

$$\hat{U}_{\text{KC}} = \hat{U}_0 e^{-ig(\hat{G}_0(T) + \hat{G}_e)} \hat{U}_{\frac{\pi}{2}}, \quad (\text{B14})$$

where $\hat{U}_0 = \hat{U}_{\frac{\pi}{2}}^{\phi_3} e^{-i\frac{T_2}{\hbar}\frac{\hat{\mathbf{p}}^2}{2m}} \hat{U}_{\pi}^{\phi_2} e^{-i\frac{T_1}{\hbar}\frac{\hat{\mathbf{p}}^2}{2m}}$ is independent of g . The state of the particle after interrogation time T is therefore

$$|\Psi(T)\rangle = \hat{U}_{\text{KC}} |\Psi_0\rangle = \hat{U}_0 e^{-ig(\hat{G}_0(T) + \hat{G}_e)} |\Psi'_0\rangle, \quad (\text{B15})$$

which is Eq. (8). Taking the derivative with respect to g gives

$$\langle \partial_g \Psi(T) | \partial_g \Psi(T) \rangle = \langle \Psi'_0 | (\hat{G}_0(T) + \hat{G}_e)^2 | \Psi'_0 \rangle, \quad (\text{B16a})$$

$$\langle \Psi(T) | \partial_g \Psi(T) \rangle = -i \langle \Psi'_0 | (\hat{G}_0(T) + \hat{G}_e) | \Psi'_0 \rangle. \quad (\text{B16b})$$

The QFI is therefore

$$F_Q^{\text{KC}} = 4\text{Var}(\hat{G}_0(T) + \hat{G}_e), \quad (\text{B17})$$

where the variance is taken with respect to $|\Psi'_0\rangle$. We use Eq. (B2) to relate this to expectations taken with respect to the initial state $|\Psi_0\rangle$:

$$F_Q^{\text{KC}} = 4\text{Var}(\hat{G}_0(T)) + \frac{1}{4}k_0^2 (T^2 - 2T_2^2)^2, \quad (\text{B18})$$

which is Eq. (10).

Appendix C: $F_C(\hat{S}_z)$ of KC interferometer

To calculate the CFI $F_C(\hat{S}_z)$ [Eq. (14)], we need to determine expressions for the probabilities $P_a(T)$ and $P_b(T)$ that the particle is detected in state $|a\rangle$ and $|b\rangle$, respectively, at the interferometer output. This first requires expressing \hat{U}_{KC} in a more convenient form. To begin, we use Eq. (B4) with $\hat{X} = -i\frac{T_2}{\hbar}\frac{\hat{\mathbf{p}}^2}{2m}$ and $\hat{Y}_{\pm} = \pm ik_0\hat{z}$ to obtain

$$e^{-i\frac{T_2}{\hbar}\frac{\hat{\mathbf{p}}^2}{2m}} e^{\pm ik_0\hat{z}} = e^{\pm ik_0\hat{z}} e^{-i\frac{T_2}{\hbar}\frac{\hat{\mathbf{p}}^2}{2m}} e^{\mp i\frac{k_0 T_2}{m} \hat{p}_z} e^{-i\frac{\hbar k_0^2 T_2}{2m}}, \quad (\text{C1})$$

where we used $[\hat{X}, \hat{Y}_{\pm}] = \mp\frac{ik_0 T_2}{m} \hat{p}_z$ and $[\hat{Y}_{\pm}, [\hat{X}, \hat{Y}_{\pm}]] = \frac{i\hbar k_0^2 T_2}{m}$. This allows us to commute $e^{-i\frac{T_2}{\hbar}\frac{\hat{\mathbf{p}}^2}{2m}}$ and $\hat{U}_{\pi}^{\phi_2}$:

$$e^{-i\frac{T_2}{\hbar}\frac{\hat{\mathbf{p}}^2}{2m}} \hat{U}_{\pi}^{\phi_2} = \hat{U}_{\pi}^{\phi_2} e^{-i\frac{T_2}{\hbar}\frac{\hat{\mathbf{p}}^2}{2m}} e^{-2i\frac{k_0 T_2}{m} \hat{p}_z \hat{S}_z} e^{-i\frac{\hbar k_0^2 T_2}{2m}}, \quad (\text{C2})$$

where we have again used Eq. (B7). Neglecting the global phase factor $\exp[-i\hbar k_0^2 T_2/(2m)]$, we can therefore write Eq. (B14) in the convenient form

$$\hat{U}_{\text{KC}} = \hat{U}_{\text{int}} \hat{U}_{\text{ext}} \hat{U}_{\frac{\pi}{2}}^{\phi_1}, \quad (\text{C3})$$

where

$$\hat{U}_{\text{int}} \equiv \hat{U}_{\frac{\pi}{2}}^{\phi_3} \hat{U}_{\pi}^{\phi_2} e^{-2i\frac{k_0 T_2}{m} \hat{p}_z \hat{S}_z} e^{-ig\hat{G}_e}, \quad (\text{C4})$$

$$\hat{U}_{\text{ext}} \equiv e^{-i\frac{T}{\hbar}\frac{\hat{\mathbf{p}}^2}{2m}} e^{-ig\hat{G}_0(T)}. \quad (\text{C5})$$

\hat{U}_{ext} only acts on the external (i.e. motional) degrees of freedom, whereas \hat{U}_{int} acts on *both* the internal and motional degrees of freedom. Note that \hat{U}_{int} and \hat{U}_{ext} do not commute.

The state of the particle at the output of the interferometer after interrogation time T is therefore

$$\begin{aligned} |\Psi(T)\rangle &= \hat{U}_{\text{int}} \hat{U}_{\text{ext}} \hat{U}_{\frac{\pi}{2}}^{\phi_1} |\Psi_0\rangle \\ &= \frac{1}{\sqrt{2}} \left(\hat{U}_{\text{int}} |a\rangle \hat{U}_{\text{ext}} |\psi_0\rangle - i \hat{U}_{\text{int}} |b\rangle \hat{U}_{\text{ext}} e^{i(k_0\hat{z}-\phi_1)} |\psi_0\rangle \right). \end{aligned} \quad (\text{C6})$$

From Eq. (7) we get:

$$\begin{aligned} \hat{U}_{\frac{\pi}{2}}^{\phi_3} \hat{U}_{\pi}^{\phi_2} &= -\frac{1}{\sqrt{2}} \left(e^{-i(\phi_2-\phi_3)} |a\rangle \langle a| + e^{i(\phi_2-\phi_3)} |b\rangle \langle b| \right) \\ &\quad - \frac{i}{\sqrt{2}} \left(e^{-i(k_0\hat{z}-\phi_2)} |a\rangle \langle b| + e^{i(k_0\hat{z}-\phi_2)} |b\rangle \langle a| \right), \end{aligned} \quad (\text{C7})$$

where ϕ_2 and ϕ_3 are the phases of the second and the third laser pulses, respectively. Using this and Eq. (B7), we obtain

$$\begin{aligned} \hat{U}_{\text{int}} |a\rangle &= -\frac{1}{\sqrt{2}} \left[e^{-i(\phi_2-\phi_3)} |a\rangle + i e^{i(k_0\hat{z}-\phi_2)} |b\rangle \right] \\ &\quad \times e^{-i\frac{k_0 T_2}{m} \hat{p}_z} e^{-ig\frac{k_0 T_2^2}{2}}, \end{aligned} \quad (\text{C8a})$$

$$\begin{aligned} \hat{U}_{\text{int}} |b\rangle &= -\frac{1}{\sqrt{2}} \left[e^{i(\phi_2-\phi_3)} |b\rangle + i e^{-i(k_0\hat{z}-\phi_2)} |a\rangle \right] \\ &\quad \times e^{i\frac{k_0 T_2}{m} \hat{p}_z} e^{ig\frac{k_0 T_2^2}{2}}. \end{aligned} \quad (\text{C8b})$$

Substituting Eqs. (C8) into Eq. (C6) gives

$$\begin{aligned} |\Psi(T)\rangle &= -\frac{1}{2} \left[\left(e^{-i(\phi_2-\phi_3)} e^{-i\frac{k_0 T_2}{m} \hat{p}_z} e^{-ig\frac{k_0 T_2^2}{2}} \hat{U}_{\text{ext}} |\psi_0\rangle + e^{-i(k_0\hat{z}-\phi_2)} e^{i\frac{k_0 T_2}{m} \hat{p}_z} e^{\frac{i}{2}gk_0 T_2^2} \hat{U}_{\text{ext}} e^{i(k_0\hat{z}-\phi_1)} |\psi_0\rangle \right) |a\rangle \right. \\ &\quad \left. + i \left(e^{i(k_0\hat{z}-\phi_2)} e^{-i\frac{k_0 T_2}{m} \hat{p}_z} e^{-ig\frac{k_0 T_2^2}{2}} \hat{U}_{\text{ext}} |\psi_0\rangle - e^{i(\phi_2-\phi_3)} e^{i\frac{k_0 T_2}{m} \hat{p}_z} e^{\frac{i}{2}gk_0 T_2^2} \hat{U}_{\text{ext}} e^{i(k_0\hat{z}-\phi_1)} |\psi_0\rangle \right) |b\rangle \right]. \end{aligned} \quad (\text{C9})$$

Defining $|\Psi_a(T)\rangle \equiv \langle a|\Psi(T)\rangle$, the probability of finding the particle in the internal state $|a\rangle$ at the output port of the interferometer is

$$\begin{aligned} P_a(T) &= \langle \Psi_a(T) | \Psi_a(T) \rangle \\ &= \frac{1}{2}[1 + \frac{1}{2}(e^{i(gk_0T_2^2 - \Phi)}\langle \psi_0 | \hat{Q} | \psi_0 \rangle + \text{h.c.})], \end{aligned} \quad (\text{C10})$$

where $\Phi \equiv \phi_1 - 2\phi_2 + \phi_3$ and

$$\begin{aligned} \hat{Q} &\equiv e^{ig\hat{G}_0(T)} e^{i\frac{T}{\hbar}\frac{\hat{p}^2}{2m}} e^{ik_0\frac{T_2}{m}\hat{p}_z} e^{-ik_0\hat{z}} \\ &\times e^{i\frac{k_0T_2}{m}\hat{p}_z} e^{-i\frac{T}{\hbar}\frac{\hat{p}^2}{2m}} e^{-ig\hat{G}_0(T)} e^{ik_0\hat{z}}, \\ &= e^{i\frac{\hbar k_0^2}{2m}(T_2 - T_1)} e^{-igk_0T(T_2 - T_1)} e^{-ig\frac{k_0T^2}{2}} e^{i\frac{k_0}{m}(T_2 - T_1)\hat{p}_z}. \end{aligned} \quad (\text{C11})$$

This final simplification follows from repeated application of Eq. (B4), and allows us to express the probability as

$$\begin{aligned} P_a(T) &= \frac{1}{2}\left[1 + \frac{1}{2}\left(e^{-i\Phi} e^{i\frac{\hbar k_0^2}{2m}(T_2 - T_1)} e^{-igk_0(\frac{T^2}{2} - T_1^2)} \right.\right. \\ &\left.\left.\times \langle \psi_0 | e^{i\frac{k_0}{m}(T_2 - T_1)\hat{p}_z} | \psi_0 \rangle + \text{h.c.}\right)\right]. \end{aligned} \quad (\text{C12})$$

If we choose the phases of our laser pulses such that $\phi_1 = \phi_2 = 0$, $\phi_3 = \pi/2$, thereby operating at the point of maximum sensitivity, we can express the probabilities in the following way:

$$P_a(T) = \frac{1}{2}\left[1 - \frac{i}{2}\left(\mathcal{C}e^{i(\phi_f - \phi_g)} - \mathcal{C}^*e^{-i(\phi_f - \phi_g)}\right)\right], \quad (\text{C13a})$$

$$P_b(T) = \frac{1}{2}\left[1 + \frac{i}{2}\left(\mathcal{C}e^{i(\phi_f - \phi_g)} - \mathcal{C}^*e^{-i(\phi_f - \phi_g)}\right)\right], \quad (\text{C13b})$$

where

$$\phi_f \equiv \frac{\hbar k_0^2}{2m}(T_2 - T_1), \quad (\text{C14a})$$

$$\phi_g \equiv k_0 g \left(\frac{T^2}{2} - T_1^2\right), \quad (\text{C14b})$$

$$\mathcal{C} \equiv \langle \psi_0 | e^{i\frac{k_0}{m}(T_2 - T_1)\hat{p}_z} | \psi_0 \rangle. \quad (\text{C14c})$$

ϕ_f represents the phase difference due to the non-symmetrical free evolution of the wavepackets in the two arms of the interferometer, while ϕ_g is the phase difference due to gravity. Expressing $\mathcal{C} = |\mathcal{C}|e^{i\vartheta}$ allows us to write Eq. (C13) in the simplified form of Eqs. (13). Here $|\mathcal{C}|$ is interpreted as a *fringe contrast* and $\alpha = \phi_f - \phi_g + \vartheta$ denotes the total phase shift.

If we measure the population difference of the two internal states, \hat{S}_z , at the output of the interferometer, the CFI is given by

$$F_C(\hat{S}_z) = \sum_{j=a,b} \frac{(\partial_g P_j)^2}{P_j} = \frac{(\partial_g P_a)^2}{P_a P_b}, \quad (\text{C15})$$

where the last equality follows from the relation $P_a + P_b = 1 \Rightarrow \partial_g P_a = -\partial_g P_b$. Noting that

$$P_a(T)P_b(T) = \frac{1}{4}\left(1 - |\mathcal{C}|^2 \sin^2 \alpha\right), \quad (\text{C16a})$$

$$\partial_g P_a(T) = -\frac{1}{2}|\mathcal{C}|k_0 \left(\frac{T^2}{2} - T_1^2\right) \cos \alpha, \quad (\text{C16b})$$

we arrive at Eq. (14).

Appendix D: Beam splitter transformation: Derivation of Eq. (7).

A Raman beam splitter is typically modelled by the Hamiltonian

$$\hat{H}_{\text{BS}} = \frac{\hat{\mathbf{p}}^2}{2m} - \hbar\delta|b\rangle\langle b| + \frac{\hbar\Omega}{2}(|b\rangle\langle a|e^{i(k_0\hat{z}-\phi)} + \text{h.c.}), \quad (\text{D1})$$

where δ is the two-photon detuning and $\Omega = \Omega_1\Omega_2/\Delta$ is the effective two-photon Rabi frequency, which depends on the single-photon Rabi frequencies $\Omega_{1,2}$ and the single-photon detuning Δ [86, 87]. The two-photon detuning is typically set to the two-photon resonance condition $\delta = \hbar k_0^2/(2m)$. Evolution under this Hamiltonian for a duration Δt is given by the unitary time-evolution operator

$$\begin{aligned} U_\theta^\phi &= \exp\left[\frac{-i\Delta t}{\hbar}\hat{H}_{\text{BS}}\right] \\ &= e^{-i\left(\frac{\hat{\mathbf{p}}^2}{2m\hbar} - \frac{\hbar k_0^2}{2m}\right)|b\rangle\langle b|} e^{\frac{\theta}{\Omega}} e^{-i\frac{\theta}{2}(|b\rangle\langle a|e^{i(k_0\hat{z}-\phi)} + \text{h.c.})}, \end{aligned} \quad (\text{D2})$$

where we have defined $\theta = \Omega\Delta t$. If $\hbar\Omega$ is significantly greater than the spread in kinetic energy of the initial state, we can ignore the first term and obtain

$$\begin{aligned} U_\theta^\phi &= \exp\left[-i\frac{\theta}{2}\left(|b\rangle\langle a|e^{i(k_0\hat{z}-\phi)} + \text{h.c.}\right)\right] \\ &= \hat{1} \cos\left(\frac{\theta}{2}\right) - i(|b\rangle\langle a|e^{i(k_0\hat{z}-\phi)} + \text{h.c.}) \sin\left(\frac{\theta}{2}\right) \end{aligned} \quad (\text{D3})$$

which is Eq. (7).

Figure 5 shows the QFI and CFI when the evolution due to the beam splitter and mirror pulses is treated as Schrödinger evolution under Hamiltonian Eq. (D1). This evolution was solved numerically for different values of Δt . We used the same initial state as Fig. 2(a). We set Ω such that $\Omega\Delta t = \pi/2$ for the two beam splitter pulses, and the duration of the interaction was doubled for the mirror pulse, resulting in $\Omega(2\Delta t) = \pi$. We find excellent agreement with the ideal beam splitter case as long as $\Delta t \ll T_\pi$. In the regime $\Delta t \sim T_\pi$, there is significant motional dynamics during the beam splitter period, and our approximation is no longer valid. For example, for the maximum value of Δt simulated ($\Delta t = 0.4T_\pi$), the total interferometer sequence time, which is the time from the commencement of the first beam splitter to the conclusion of the second beam splitter, is $3.6T_\pi$ (compared to $2T_\pi$ for instantaneous beam splitters). For typical experiments, such as Ref. [7], $\Delta t/T_\pi \sim 10^{-4}$.

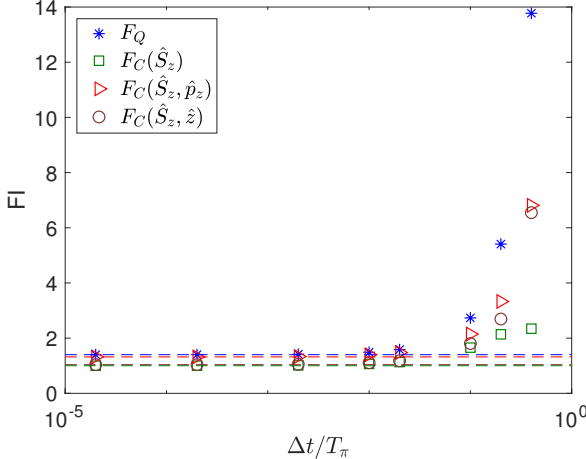


FIG. 5. (a) QFI and CFI computed using Eq. (D1) rather than Eq. (D3) as a function of Δt . Provided $\Delta t/T_\pi \ll 1$, Eq. (D3) (shown by dashed lines of the appropriate colour) is an excellent approximation to the true dynamics. Fisher information is presented in units of $k_0^2 T_\pi^4$.

- [1] Achim Peters, Keng Yeow Chung, and Steven Chu, “Measurement of gravitational acceleration by dropping atoms,” *Nature* **400**, 849–852 (1999).

[2] A Peters, K Y Chung, and S Chu, “High-precision gravity measurements using atom interferometry,” *Metrologia* **38**, 25 (2001).

[3] Zhong-Kun Hu, Bu-Liang Sun, Xiao-Chun Duan, Min-Kang Zhou, Le-Le Chen, Su Zhan, Qiao-Zhen Zhang, and Jun Luo, “Demonstration of an ultrahigh-sensitivity atom-interferometry absolute gravimeter,” *Phys. Rev. A* **88**, 043610 (2013).

[4] M. Hauth, C. Freier, V. Schkolnik, A. Senger, M. Schmidt, and A. Peters, “First gravity measurements using the mobile atom interferometer gain,” *Applied Physics B* **113**, 49–55 (2013).

[5] P A Altin, M T Johnsson, V Negnevitsky, G R Dennis, R P Anderson, J E Debs, S S Szigeti, K S Hardman, S Bennetts, G D McDonald, L D Turner, J D Close, and N P Robins, “Precision atomic gravimeter based on bragg diffraction,” *New Journal of Physics* **15**, 023009 (2013).

[6] C Freier, M Hauth, V Schkolnik, B Leykauf, M Schilling, H Wziontek, H-G Scherneck, J Müller, and A Peters, “Mobile quantum gravity sensor with unprecedented stability,” *Journal of Physics: Conference Series* **723**, 012050 (2016).

[7] K. S. Hardman, P. J. Everitt, G. D. McDonald, P. Manju, P. B. Wigley, M. A. Sooriyabandara, C. C. N. Kuhn, J. E. Debs, J. D. Close, and N. P. Robins, “Simultaneous precision gravimetry and magnetic gradiometry with a bose-einstein condensate: A high precision, quantum sensor,” *Phys. Rev. Lett.* **117**, 138501 (2016).

[8] M. J. Snadden, J. M. McGuirk, P. Bouyer, K. G. Haritos, and M. A. Kasevich, “Measurement of the earth’s gravity gradient with an atom interferometer-based gravity gradiometer,” *Phys. Rev. Lett.* **81**, 971–974 (1998).

[9] G. Stern, B. Battelier, R. Geiger, G. Varoquaux, A. Villing, F. Moron, O. Carraz, N. Zahzam, Y. Bidel, W. Chaibi, F. Pereira Dos Santos, A. Bresson, A. Landragin, and P. Bouyer, “Light-pulse atom interferometry in microgravity,” *The European Physical Journal D* **53**, 353–357 (2009).

[10] F. Sorrentino, Q. Bodart, L. Cacciapuoti, Y.-H. Lien, M. Prevedelli, G. Rosi, L. Salvi, and G. M. Tino, “Sensitivity limits of a raman atom interferometer as a gravity gradiometer,” *Phys. Rev. A* **89**, 023607 (2014).

[11] G. W. Biedermann, X. Wu, L. Deslauriers, S. Roy, C. Ma-hadeswaraswamy, and M. A. Kasevich, “Testing gravity with cold-atom interferometers,” *Phys. Rev. A* **91**, 033629 (2015).

[12] G. D’Amico, F. Borselli, L. Cacciapuoti, M. Prevedelli, G. Rosi, F. Sorrentino, and G. M. Tino, “Bragg interferometer for gravity gradient measurements,” *Phys. Rev. A* **93**, 063628 (2016).

[13] Peter Asenbaum, Chris Overstreet, Tim Kovachy, Daniel D. Brown, Jason M. Hogan, and Mark A. Kasevich, “Phase shift in an atom interferometer due to spacetime curvature across its wave function,” *Phys. Rev. Lett.* **118**, 183602 (2017).

[14] Y. Bidel, N. Zahzam, C. Blanchard, A. Bonnin, M. Cadoret, A. Bresson, D. Rouxel, and M. F. Lequentrec-Lalancette, “Absolute marine gravimetry with matter-wave interferometry,” *Nature Communications* **9**, 627 (2018).

[15] Justin Arthur Richeson, *Gravity Gradiometer Aided Inertial Navigation Within Non-GNSS Environments*, Ph.D. thesis, University of Maryland (2008).

[16] M. I. Evstifeev, “The state of the art in the development of onboard gravity gradiometers,” *Gyroscopy and Navigation* **1**, 1–12 (2017).

- gation **8**, 68–79 (2017).
- [17] Sebastian Fray, Cristina Alvarez Diez, Theodor W. Hänsch, and Martin Weitz, “Atomic interferometer with amplitude gratings of light and its applications to atom based tests of the equivalence principle,” Phys. Rev. Lett. **93**, 240404 (2004).
- [18] Savas Dimopoulos, Peter W. Graham, Jason M. Hogan, and Mark A. Kasevich, “Testing general relativity with atom interferometry,” Phys. Rev. Lett. **98**, 111102 (2007).
- [19] D. Schlippert, J. Hartwig, H. Albers, L. L. Richardson, C. Schubert, A. Roura, W. P. Schleich, W. Ertmer, and E. M. Rasel, “Quantum test of the universality of free fall,” Phys. Rev. Lett. **112**, 203002 (2014).
- [20] Giovanni Amelino-Camelia, Claus Lämmerzahl, Flavio Mercati, and Guglielmo M. Tino, “Constraining the energy-momentum dispersion relation with planck-scale sensitivity using cold atoms,” Phys. Rev. Lett. **103**, 171302 (2009).
- [21] Dongfeng Gao and Mingsheng Zhan, “Constraining the generalized uncertainty principle with cold atoms,” Phys. Rev. A **94**, 013607 (2016).
- [22] Ch.J. Bordé, “Atomic interferometry with internal state labelling,” Physics Letters A **140**, 10 – 12 (1989).
- [23] Mark Kasevich and Steven Chu, “Atomic interferometry using stimulated raman transitions,” Phys. Rev. Lett. **67**, 181–184 (1991).
- [24] M. Kasevich and S. Chu, “Measurement of the gravitational acceleration of an atom with a light-pulse atom interferometer,” Applied Physics B: Lasers and Optics **54**, 321–332 (1992).
- [25] Pippa Storey and Claude Cohen-Tannoudji, “The feynman path integral approach to atomic interferometry. a tutorial,” Journal de Physique II **4**, 1999–2027 (1994).
- [26] Wolfgang P. Schleich, Daniel M. Greenberger, and Ernst M. Rasel, “Redshift controversy in atom interferometry: Representation dependence of the origin of phase shift,” Phys. Rev. Lett. **110**, 010401 (2013).
- [27] Wolfgang P Schleich, Daniel M Greenberger, and Ernst M Rasel, “A representation-free description of the Kasevich–Chu interferometer: a resolution of the redshift controversy,” New Journal of Physics **15**, 013007 (2013).
- [28] Holger Müller, Sheng-wei Chiow, Quan Long, Sven Herrmann, and Steven Chu, “Atom interferometry with up to 24-photon-momentum-transfer beam splitters,” Phys. Rev. Lett. **100**, 180405 (2008).
- [29] Pierre Cladé, Saïda Guellati-Khélifa, François Nez, and François Biraben, “Large momentum beam splitter using bloch oscillations,” Phys. Rev. Lett. **102**, 240402 (2009).
- [30] Sheng-wei Chiow, Tim Kovachy, Hui-Chun Chien, and Mark A. Kasevich, “ $102\hbar k$ large area atom interferometers,” Phys. Rev. Lett. **107**, 130403 (2011).
- [31] G. D. McDonald, C. C. N. Kuhn, S. Bennetts, J. E. Debs, K. S. Hardman, M. Johnsson, J. D. Close, and N. P. Robins, “ $80\hbar k$ momentum separation with bloch oscillations in an optically guided atom interferometer,” Phys. Rev. A **88**, 053620 (2013).
- [32] T. Mazzoni, X. Zhang, R. Del Aguilal, L. Salvi, N. Poli, and G. M. Tino, “Large-momentum-transfer bragg interferometer with strontium atoms,” Phys. Rev. A **92**, 053619 (2015).
- [33] C. Gross, T. Zibold, E. Nicklas, J. Estève, and M. K. Oberthaler, “Nonlinear atom interferometer surpasses classical precision limit,” Nature **464**, 1165–1169 (2010).
- [34] B. Lücke, M. Scherer, J. Kruse, L. Pezzé, F. Deuretzbacher, P. Hyllus, O. Topic, J. Peise, W. Ertmer, J. Arlt, L. Santos, A. Smerzi, and C. Klemp, “Twin matter waves for interferometry beyond the classical limit,” Science **334**, 773–776 (2011).
- [35] D. Linnemann, H. Strobel, W. Muessel, J. Schulz, R. J. Lewis-Swan, K. V. Kheruntsyan, and M. K. Oberthaler, “Quantum-enhanced sensing based on time reversal of nonlinear dynamics,” Phys. Rev. Lett. **117**, 013001 (2016).
- [36] Onur Hosten, Nils J. Engelsen, Rajiv Krishnakumar, and Mark A. Kasevich, “Measurement noise 100 times lower than the quantum-projection limit using entangled atoms,” Nature **529**, 505–508 (2016).
- [37] G. Colangelo, F. Martin Ciurana, G. Puentes, M. W. Mitchell, and R. J. Sewell, “Entanglement-enhanced phase estimation without prior phase information,” Phys. Rev. Lett. **118**, 233603 (2017).
- [38] J. E. Debs, P. A. Altin, T. H. Barter, D. Döring, G. R. Dennis, G. McDonald, R. P. Anderson, J. D. Close, and N. P. Robins, “Cold-atom gravimetry with a Bose-Einstein condensate,” Phys. Rev. A **84**, 033610 (2011).
- [39] Anne Louchet-Chauvet, Tristan Farah, Quentin Bodart, André Clairon, Arnaud Landragin, Sébastien Merlet, and Franck Pereira Dos Santos, “The influence of transverse motion within an atomic gravimeter,” New Journal of Physics **13**, 065025 (2011).
- [40] S S Szigeti, J E Debs, J J Hope, N P Robins, and J D Close, “Why momentum width matters for atom interferometry with bragg pulses,” New Journal of Physics **14**, 023009 (2012).
- [41] Kyle S. Hardman, Carlos C. N. Kuhn, Gordon D. McDonald, John E. Debs, Shayne Bennetts, John D. Close, and Nicholas P. Robins, “Role of source coherence in atom interferometry,” Phys. Rev. A **89**, 023626 (2014).
- [42] N. P. Robins, P. A. Altin, J. E. Debs, and J. D. Close, “Atom lasers: Production, properties and prospects for precision inertial measurement,” Physics Reports **529**, 265–296 (2013).
- [43] S. S. Szigeti, M. R. Hush, A. R. R. Carvalho, and J. J. Hope, “Continuous measurement feedback control of a bose-einstein condensate using phase-contrast imaging,” Physical Review A **80**, 013614 (2009).
- [44] S. S. Szigeti, M. R. Hush, A. R. R. Carvalho, and J. J. Hope, “Feedback control of an interacting bose-einstein condensate using phase-contrast imaging,” Phys. Rev. A **82**, 043632 (2010).
- [45] M R Hush, S S Szigeti, A R R Carvalho, and J J Hope, “Controlling spontaneous-emission noise in measurement-based feedback cooling of a bose-einstein condensate,” New Journal of Physics **15**, 113060 (2013).
- [46] P A Altin, G McDonald, D Döring, J E Debs, T H Barter, J D Close, N P Robins, S A Haine, T M Hanna, and R P Anderson, “Optically trapped atom interferometry using the clock transition of large 87rb bose-einstein condensates,” New Journal of Physics **13**, 065020 (2011).
- [47] S. A. Haine and A. J. Ferris, “Surpassing the standard quantum limit in an atom interferometer with four-mode entanglement produced from four-wave mixing,” Phys. Rev. A **84**, 043624 (2011).
- [48] S. A. Haine, “Information-recycling beam splitters for quantum enhanced atom interferometry,” Phys. Rev. Lett. **110**, 053002 (2013).
- [49] S. A. Haine, J. Lau, R. P. Anderson, and M. T. Johnsson,

- "Self-induced spatial dynamics to enhance spin squeezing via one-axis twisting in a two-component bose-einstein condensate," Phys. Rev. A **90**, 023613 (2014).
- [50] Stuart S. Szigeti, Behnam Tonekaboni, Wing Yung S. Lau, Samantha N. Hood, and Simon A. Haine, "Squeezed-light-enhanced atom interferometry below the standard quantum limit," Phys. Rev. A **90**, 063630 (2014).
- [51] Behnam Tonekaboni, Simon A. Haine, and Stuart S. Szigeti, "Heisenberg-limited metrology with a squeezed vacuum state, three-mode mixing, and information recycling," Phys. Rev. A **91**, 033616 (2015).
- [52] Simon A. Haine, Stuart S. Szigeti, Matthias D. Lang, and Carlton M. Caves, "Heisenberg-limited metrology with information recycling," Phys. Rev. A **91**, 041802 (2015).
- [53] Simon A. Haine and Stuart S. Szigeti, "Quantum metrology with mixed states: When recovering lost information is better than never losing it," Phys. Rev. A **92**, 032317 (2015).
- [54] Samuel P. Nolan, Jacopo Sabbatini, Michael W. J. Bromley, Matthew J. Davis, and Simon A. Haine, "Quantum enhanced measurement of rotations with a spin-1 bose-einstein condensate in a ring trap," Phys. Rev. A **93**, 023616 (2016).
- [55] Simon A. Haine and Wing Yung Sarah Lau, "Generation of atom-light entanglement in an optical cavity for quantum enhanced atom interferometry," Phys. Rev. A **93**, 023607 (2016).
- [56] Stuart S. Szigeti, Robert J. Lewis-Swan, and Simon A. Haine, "Pumped-up $su(1,1)$ interferometry," Phys. Rev. Lett. **118**, 150401 (2017).
- [57] Simon A Haine, "Quantum noise in bright soliton matter-wave interferometry," New Journal of Physics **20**, 033009 (2018).
- [58] Shau-Yu Lan, Pei-Chen Kuan, Brian Estey, Philipp Haslinger, and Holger Müller, "Influence of the coriolis force in atom interferometry," Phys. Rev. Lett. **108**, 090402 (2012).
- [59] V. Schkolnik, B. Leykauf, M. Hauth, C. Freier, and A. Peters, "The effect of wavefront aberrations in atom interferometry," Applied Physics B **120**, 311–316 (2015).
- [60] Samuel L. Braunstein and Carlton M. Caves, "Statistical distance and the geometry of quantum states," Phys. Rev. Lett. **72**, 3439–3443 (1994).
- [61] Rafał Demkowicz-Dobrzański, M. Jarzyna, and J. Kołodyński, "Quantum limits in optical interferometry," Progress in Optics **345** (2015).
- [62] Géza Tóth and Iagoba Apellaniz, "Quantum metrology from a quantum information science perspective," Journal of Physics A: Mathematical and Theoretical **47**, 424006 (2014).
- [63] Simon A. Haine, "Mean-field dynamics and fisher information in matter wave interferometry," Phys. Rev. Lett. **116**, 230404 (2016).
- [64] Sofia Qvarfort, Alessio Serafini, Peter Barker, and Sougato Bose, "Gravimetry through non-linear optomechanics," arXiv:1706.09131 ((2017)).
- [65] M. R. Matthews, B. P. Anderson, P. C. Haljan, D. S. Hall, M. J. Holland, J. E. Williams, C. E. Wieman, and E. A. Cornell, "Watching a superfluid untwist itself: Recurrence of rabi oscillations in a bose-einstein condensate," Phys. Rev. Lett. **83**, 3358–3361 (1999).
- [66] Hubert Ammann and Nelson Christensen, "Delta kick cooling: A new method for cooling atoms," Phys. Rev. Lett. **78**, 2088–2091 (1997).
- [67] Luca Pezzé and Augusto Smerzi, "Ultrasensitive two-mode interferometry with single-mode number squeezing," Phys. Rev. Lett. **110**, 163604 (2013).
- [68] Marco Gabbrielli, Luca Pezzè, and Augusto Smerzi, "Spin-mixing interferometry with bose-einstein condensates," Phys. Rev. Lett. **115**, 163002 (2015).
- [69] Samuel P. Nolan, Stuart S. Szigeti, and Simon A. Haine, "Optimal and robust quantum metrology using interaction-based readouts," Phys. Rev. Lett. **119**, 193601 (2017).
- [70] S. S. Mirkhalaf, S. P. Nolan, and S. A. Haine, "Robustifying twist-and-turn entanglement with interaction-based readout," arXiv:1803.08789 (2018).
- [71] Simon A. Haine, "Using interaction-based readouts to approach the ultimate limit of detection noise robustness for quantum-enhanced metrology in collective spin systems," arXiv:1806.00057 (2018).
- [72] Igor Gotlibovych, Tobias F. Schmidutz, Alexander L. Gaunt, Nir Navon, Robert P. Smith, and Zoran Hadzibabic, "Observing properties of an interacting homogeneous bose-einstein condensate: Heisenberg-limited momentum spread, interaction energy, and free-expansion dynamics," Phys. Rev. A **89**, 061604 (2014).
- [73] W. Ketterle, D. S. Durfee, and D. M. Stamper-Kurn, "Making, probing and understanding bose-einstein condensates," in *Proceedings of the International School of Physics "Enrico Fermi"*, Vol. 140, edited by M. Inguscio, S. Stringari, and C.E. Wieman (1999) p. 67.
- [74] K. S. Hardman, P. B. Wigley, P. J. Everitt, P. Manju, C. C. N. Kuhn, and N. P. Robins, "Time-of-flight detection of ultra-cold atoms using resonant frequency modulation imaging," Opt. Lett. **41**, 2505–2508 (2016).
- [75] J. Stenger, S. Inouye, A. P. Chikkatur, D. M. Stamper-Kurn, D. E. Pritchard, and W. Ketterle, "Bragg spectroscopy of a bose-einstein condensate," Phys. Rev. Lett. **82**, 4569–4573 (1999).
- [76] S. Richard, F. Gerbier, J. H. Thywissen, M. Hugbart, P. Bouyer, and A. Aspect, "Momentum spectroscopy of 1d phase fluctuations in bose-einstein condensates," Phys. Rev. Lett. **91**, 010405 (2003).
- [77] Mattias Johnsson, Simon Haine, Joseph Hope, Nick Robins, Cristina Figl, Matthew Jeppesen, Julien Dugué, and John Close, "Semiclassical limits to the linewidth of an atom laser," Phys. Rev. A **75**, 043618 (2007).
- [78] S. S. Szigeti and S. A. Haine, in preparation.
- [79] Stefan Gerlich, Lucia Hackermuller, Klaus Hornberger, Alexander Stibor, Hendrik Ulbricht, Michael Gring, Fabienne Goldfarb, Tim Savas, Marcel Muri, Marcel Mayor, and Markus Arndt, "A kapitza-dirac-talbot-lau interferometer for highly polarizable molecules," Nat Phys **3**, 711–715 (2007).
- [80] R. E. Sapiro, R. Zhang, and G. Raithel, "Atom interferometry using kapitza-dirac scattering in a magnetic trap," Phys. Rev. A **79**, 043630 (2009).
- [81] Bryce Gadway, Daniel Pertot, René Reimann, Martin G. Cohen, and Dominik Schneble, "Analysis of kapitza-dirac diffraction patterns beyond the raman-nath regime," Opt. Express **17**, 19173–19180 (2009).
- [82] WeiDong Li, Tianchen He, and Augusto Smerzi, "Multimode kapitza-dirac interferometry with trapped cold atoms," Phys. Rev. Lett. **113**, 023003 (2014).
- [83] Tianchen He and Pengbin Niu, "Multimode kapitza-

- dirac interferometer on bose-einstein condensates with atomic interactions,” Physics Letters A **381**, 1087 – 1091 (2017).
- [84] J. Fekete, S. Chai, S. A. Gardiner, and M. F. Andersen, “Resonant transfer of large momenta from finite-duration pulse sequences,” Phys. Rev. A **95**, 033601 (2017).
- [85] V. Guarnera, R. Moore, A. Bunting, T. Vanderbruggen, and Y. B. Ovchinnikov, “Distributed quasi-bragg beam splitter in crossed atomic waveguides,” Scientific Reports **7**, 4749 (2017).
- [86] N. P. Robins, C. Figl, S. A. Haine, A. K. Morrison, M. Jeppesen, J. J. Hope, and J. D. Close, “Achieving peak brightness in an atom laser,” Phys. Rev. Lett. **96**, 140403 (2006).
- [87] Mattias T. Johnsson and Simon A. Haine, “Generating quadrature squeezing in an atom laser through self-interaction,” Phys. Rev. Lett. **99**, 010401 (2007).